

DEVELOPMENT AND CHARACTERIZATION OF THE BONDING AND INTEGRATION TECHNOLOGIES NEEDED FOR FABRICATING SILICON CARBIDE BASED INJECTOR COMPONENTS

Michael C. Halbig
Army Research Laboratory, NASA Glenn Research Center
Cleveland, OH, USA

Mrityunjay Singh
Ohio Aerospace Institute, NASA Glenn Research Center
Cleveland, OH, USA

ABSTRACT

Advanced ceramic bonding and integration technologies play a critical role in the fabrication and application of silicon carbide based components for a number of aerospace and ground based applications. One such application is a lean direct injector for a turbine engine to achieve low NOx emissions. Ceramic to ceramic diffusion bonding and ceramic to metal brazing technologies are being developed for this injector application. For the diffusion bonding technology, titanium interlayers (coatings and foils) were used to aid in the joining of silicon carbide (SiC) substrates. The influence of such variables as surface finish, interlayer thickness, and processing time were investigated. Electron microprobe analysis was used to identify the reaction formed phases. In the diffusion bonds, an intermediate phase, $Ti_2Si_2C_3$, formed that is thermally incompatible in its thermal expansion and caused thermal stresses and cracking during the processing cool-down. Thinner interlayers of pure titanium and/or longer processing times resulted in an optimized microstructure. Tensile tests on the joined materials resulted in strengths of 13-28 MPa depending on the SiC substrate material. Non-destructive evaluation using ultrasonic immersion showed well formed bonds. For the joining technology of brazing Kovar fuel tubes to silicon carbide, preliminary development of the joining approach has begun. Various technical issues and requirements for the injector application are addressed.

INTRODUCTION

Silicon carbide ceramics are a very promising material for use in high-temperature, structural applications. The beneficial properties include high creep resistance, corrosion resistance, and high temperature strength and stability over long durations. One such application is for a ceramic injector in jet engines that enables more efficient fuel combustion and lower emissions during sub-sonic and super-sonic cruise. The ceramic lean-direct injector which is to be fabricated from SiC laminates is illustrated in Figure 1. Each laminate section contains its own distinct hole pattern for channeling the fuel and combustion air separately. When the laminates are stacked in order, fluid circuits for the fuel and combustion air are formed. At the exiting surface, the fuel and combustion air mix to provide efficient combustion with low emissions and low NOx.

The diffusion bonding of SiC laminates and the brazing of Kovar tubes to SiC are enabling technologies for developing the injector. The diffusion bonding allows for the fabrication of a multilayered component with complex internal passages. The brazing technology allows the injector component to be integrated into the surrounding engine system through the adjoining fuel system. Requirements of the SiC laminate bonding technology include the ability to join relatively large, flat geometries (i.e. 10.16 cm diameter discs), leak free operation, and chemical and mechanical stability for long durations at operation conditions. Technical challenges in developing the diffusion bonding

debonding was observed. However, microcracking occurred in the diffusion bond formed with the thicker 20 micron interlayer due to the formation of the Ti_5Si_3 phase.

In the current study, processing optimization and diffusion bond characterization were the primary focus. Pure Ti interlayers (PVD coatings and foils) were down selected as the preferred interlayer. The results discussed in the previous paragraph will be presented in this paper to serve as an introduction to the characterization and processing optimization that was conducted. Additional joint fabrication was conducted using pure Ti foils in different thicknesses and at different processing times in an effort to better understand the formation of the reaction formed phases in the diffusion bond and the conditions which contributed to crack and void formation. Further characterization was conducted through non-destructive evaluation (NDE), strength tests, optical microscopy, scanning electron microscopy (SEM), and electron microprobe analysis.

EXPERIMENTAL

Silicon carbide was diffusion bonded to silicon carbide with the aid of Ti interlayers. The silicon carbide material was fabricated by Rohm & Haas through the method of chemical vapor deposition (CVD). Pure Ti was used as the interlayer. For the preliminary study (discussed in the introduction), physically vapor deposited (PVD) Ti coatings with a thickness of 10 microns were applied to the SiC substrates. In one case, coated and uncoated substrates were matched to provide a 10 micron interlayer. In another case, two coated substrates were matched to provide a 20 micron interlayer. Processing of the diffusion bonds was carried out in a hot press with an environmental chamber. The paired substrates were processed at the following conditions: 1250°C, vacuum, 31 MPa applied pressure, and a 2 hr hold, followed by a cooling rate of 2 °C per minute. The joints were analyzed using a JEOL JXA-8200 Superprobe electron microprobe to provide scanning electron microscopy and EDS analysis to identify the quality of the bonds and to identify the reaction formed phases.

In order to obtain samples for NDE and strength tests, two sets of 2.54 cm diameter discs were also bonded at the above conditions. A 10 micron thick PVD coating had been applied to the inner 1.66 cm diameter of the one of the matching discs. The two paired sets of discs had different surface finishes. In one case, the matching discs were highly polished and had a black, mirror like finish. In the other case, the matching discs were unpolished so that they had a dull, non-reflective, grey finish. The sets of discs are shown in Figure 2. Before the discs were bonded, the surfaces and applied coatings were evaluated under an optical microscope. After bonding, these sets of joined discs were non-destructively evaluated using the methods of pulsed thermography and ultrasonic immersion. Finally, the discs were fracture tested to determine the strength of the bonds. The fracture surfaces were analyzed under an optical microscope.

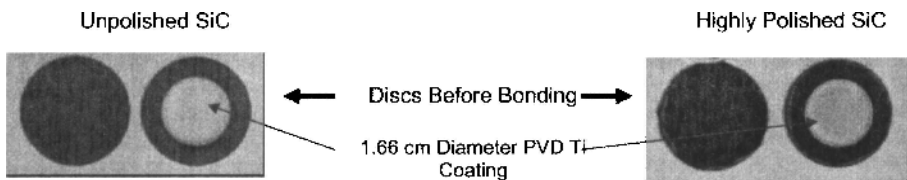


Figure 2. Photos of the coated and uncoated sets of SiC discs before bonding. The less polished discs are on the left and the more polished discs are on the right.

In another study, the effects of processing time and Ti interlayer thickness were investigated. The Ti foils were obtained from Goodfellow Corporation. The foils were placed between the SiC substrates and processing was carried out at the same conditions as above except the hold times were varied. The foil thicknesses and processing times that were investigated were 10 micron at 2 hours, 20 microns at 1, 2, and 4 hours, and 50 microns at 1, 2, 4, 8, and 16 hours. Polished cross sections of the diffusion bonds were prepared for analysis under an optical microscope. In the future, analysis with scanning electron microscopy (SEM) and electron dispersive x-ray spectrometry (EDS) will be conducted.

For a final study, a final pair of substrates (Hexoloy SiC) were bonded with a Ti foil interlayer that had a hole pattern cut out of it to simulate debonded areas. The purpose was to determine the size limitations for detecting flaws and debonds using NDE. The joined substrates were analyzed with the NDE method of ultrasonic immersion

RESULTS AND DISCUSSION

Polished cross-sections of the diffusion bonds that were formed with the PVD Ti interlayers with thicknesses of 20 microns and 10 microns are shown in Figures 3 and 4 respectively. In both cases, the reaction formed diffusion bonds are well adhered to the SiC substrates. However microcracks were observed in the diffusion bond formed with the thicker 20 micron PVD Ti interlayer. The corresponding microprobe analysis of the reaction formed phases is given in Table I. The presence of the phase, $Ti_5Si_3C_x$ (Phase C in Figure 3 and Table I), is observed which was also one of the phases believed to contribute to microcracking when the Ti-6Al-4V alloy foil was used as an interlayer^{2,3}. The $Ti_5Si_3C_x$ phase was suggested by Naka *et al.*⁶ to be an intermediate phase that will not be present when the phase reactions have gone to completion. Therefore, in our approach for forming stable fully reacted diffusion bonds, the $Ti_5Si_3C_x$ phase can be avoided in the final diffusion bond by either using a Ti interlayer that is thinner than 20 microns or by processing for longer durations. This appears to be the case as seen in the bond formed from the thinner 10 micron PVD Ti interlayer. The micrograph in Figure 4 shows a well formed diffusion bond. Two phases are present as seen from the microprobe analysis in Table II. The absence of microcracking is because the detrimental phase of Ti_5Si_3 was not present. The use of a thinner interlayer while maintaining the same processing time resulted in a stable diffusion bond with no intermediate phases. The source of the dark pores in the bond still has to be determined. It may be due to the formation of more dense phases during the diffusion bonding process. The presence of the pores may not have a significant effect on the mechanical and leakage properties of the bond, since the pores are very small and isolated. Future tests and analysis will determine if the small, isolated pores have an effect on leakage through the bonds.

The two sets of discs that were bonded were analyzed by NDE followed by strength tests. The two sets of discs that were bonded had different surface finishes as shown in Figure 2. Greater detail of the discs and coatings is shown in Figure 5. The highly polished substrate has a more dense surface which allowed for a more dense PVD coating to be applied. For the less polished substrate, the applied coating is less dense. The transition between the coated and uncoated sections on this substrate was difficult to distinguish due to the rough surface. The first NDE approach that was investigated was pulsed thermography (alternately referred to as flash thermography). A description of the pulsed thermography method is illustrated in Figure 6. Since the coating was only applied to the inner 1.66 cm diameter of the 2.54 cm diameter discs, it would be expected that NDE would detect a bonded inner diameter and a non-bonded outer ring. However, pulsed thermography was not able to clearly detect these bonded and non-bonded areas as shown in the NDE results in Figure 7. The general region where bonding was presumed to have occurred was detected; however, the image was not very sharp. The results regarding the bonding quality are inconclusive due to high surface reflectivity.

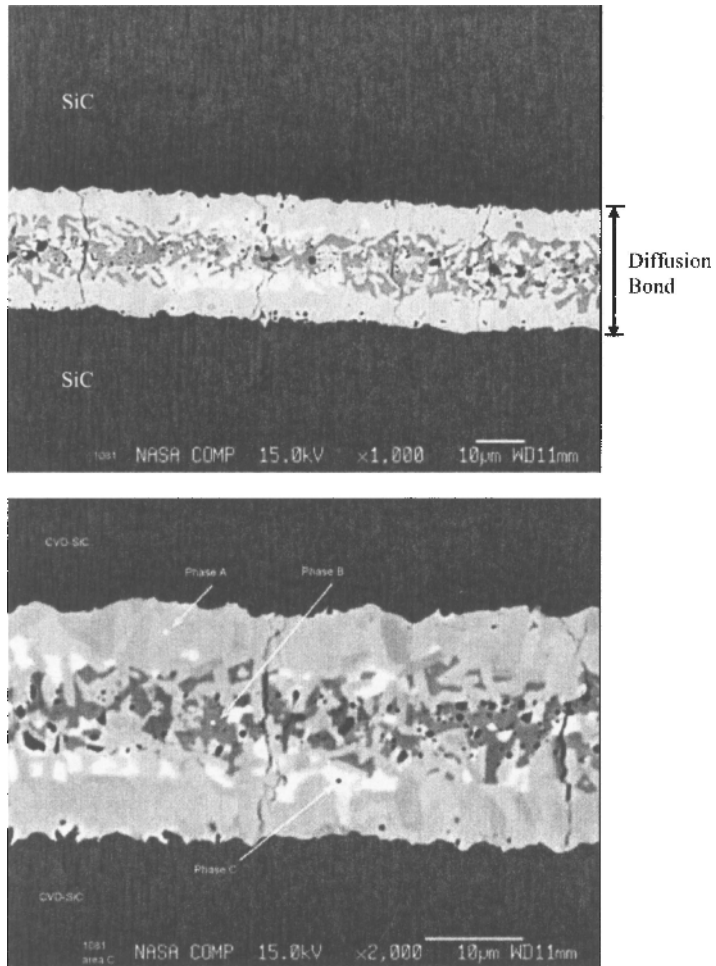


Figure 3. Diffusion bond when a 20 micron thick PVD Ti coating was used as the interlayer between the Rohm & Haas SiC substrates. The top is at a magnification of x1000 and the bottom micrograph is at a magnification of x2000. Microcracks and the presence of three phases are observed.

Table 1. Microprobe analysis of the atomic ratios for the reaction formed phases in the diffusion bond as shown in Figure 3 (atomic ratios are an average from five locations for each phase).

| Phase | Al | Fe | Ti | Si | C | Cr | Total |
|---------|-------|-------|--------|--------|--------|-------|---------|
| Phase A | 0.011 | 0.001 | 56.426 | 17.792 | 25.757 | 0.014 | 100.000 |
| Phase B | 0.007 | 0.005 | 35.784 | 62.621 | 1.570 | 0.003 | 100.000 |
| Phase C | 0.027 | 0.153 | 58.767 | 33.891 | 7.140 | 0.023 | 100.000 |

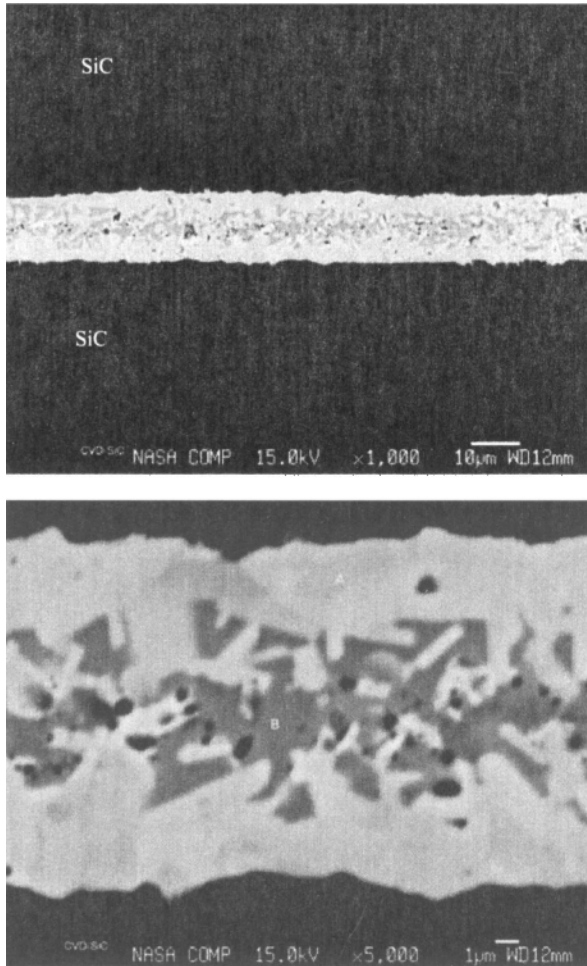


Figure 4. Diffusion bond when a 10 micron thick PVD Ti coating was used as the interlayer between the Rohm & Haas SiC substrates. The top is at a magnification of x1000 and the bottom micrograph is at a magnification of x5000. No microcracks and the presence of three phases are observed.

Table II. Microprobe analysis of the atomic ratios for the reaction formed phases in the diffusion bond as shown in Figure 4 (atomic ratios are an average from five locations for each phase).

| Phase | C | Si | Ti | Al | Cr | Total |
|---------|--------|--------|--------|-------|-------|---------|
| SiC | 45.890 | 54.096 | 0.011 | 0.000 | 0.004 | 100.000 |
| Phase A | 24.686 | 18.690 | 56.621 | - | 0.003 | 100.000 |
| Phase B | 3.028 | 61.217 | 35.752 | - | 0.003 | 100.000 |

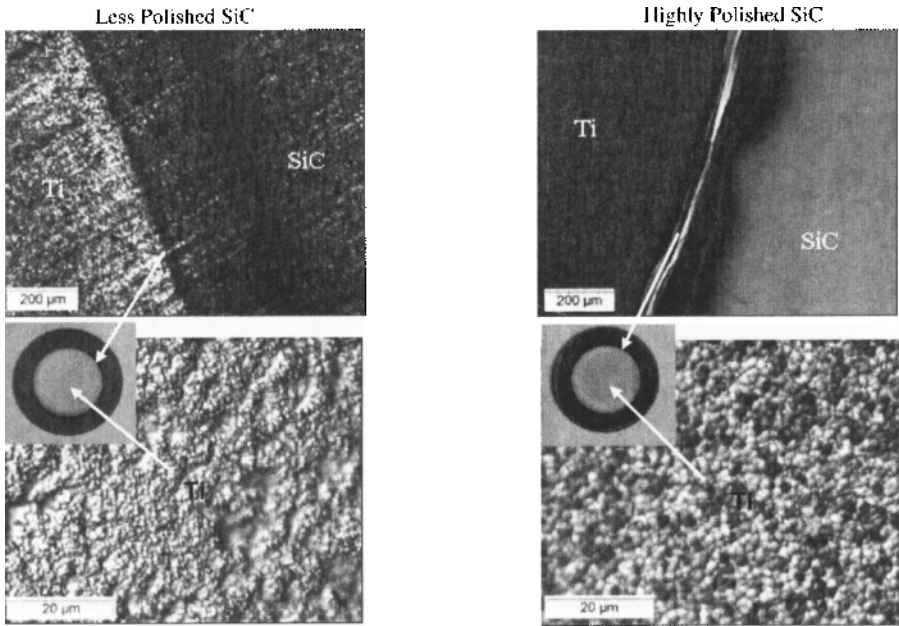


Figure 5. Optical views of the SiC substrate and PVD Ti coatings for the less polished (left) and the more polished SiC (right). Macroviews of the discs are shown for reference.

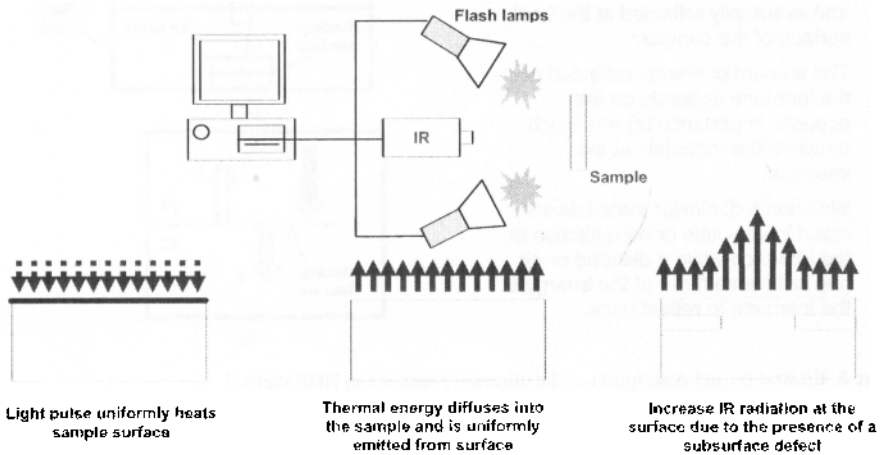


Figure 6. Illustration and description of the flash thermography NDE method.



Figure 7. Results from pulsed thermography for the less polished pair of joined substrates (left) and for the more polished pair (right).

The second method of NDE that was investigated was ultrasonic immersion. This method is illustrated and described in Figure 8. Ultrasonic immersion gave much better NDE results, as seen in Fig. 9, compared to using pulsed thermography. The inner diameter of the bonded surface and the outer ring of a non-bonded area are very clearly visible. The ultrasonic immersion results for the more polished set of substrates resulted in a sharper image than for the less polished set of substrates which appear as slightly blurred. The results suggest that the more polished substrates gave a more dense and higher quality bond.

- A high frequency ultrasonic pulse (U) enters specimen.
- Some of the signal is reflected back at the bond interface (R) while the remaining energy is transmitted (T) and eventually reflected at the back surface of the sample.
- The amount of energy reflected at the interface depends on the acoustic impedance (z) mismatch between the materials at the interface.
- Well bonded, similar materials will result in very little or no reflection at the interface while a disbond or air gap will cause more of the energy at the interface to reflect back.

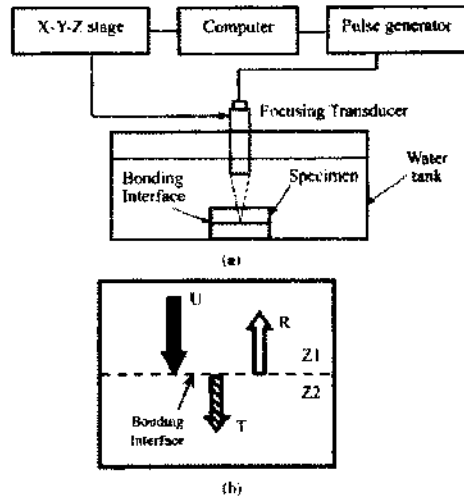


Figure 8. Illustration and description of the ultrasonic immersion NDE method.

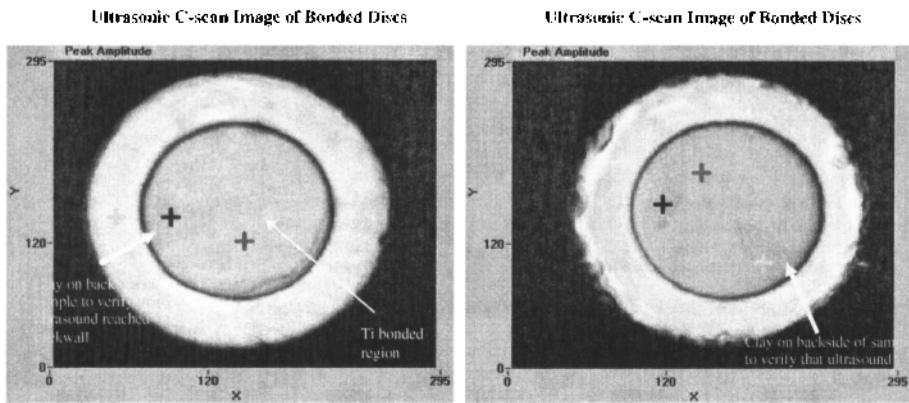


Figure 9. Results from ultrasonic immersion for the less polished pair of joined substrates (left) and for the more polished pair (right).

After completion of the NDE analysis on the two sets of joined discs, they were tensile tested and analyzed under an optical microscope. An illustration of the samples under stress is shown in Figure 10 along with the configuration for additional square samples that were previously tested. The stress versus strain curves are shown in Figure 11 for the joined discs. The less polished set of joined discs had a strength of 13.4 MPa and the more polished set had a strength of 15.0 MPa. This was lower than previous strength test of two sets of joined square SiC substrates with dimensions of 2.54 cm x 2.54 cm. The joined square substrates had strengths of greater than 23.6 MPa and 28.4 MPa. Failures occurred in the adhesives used to attach the test fixtures to the substrates. Despite the discrepancy in strengths from the two sample configurations, the strengths are much higher than those required for the application which is 3.45-6.89 MPa. The stress versus strain curves for the discs in Figure 11 show that the more polished discs had a slightly higher strength. Although the limited testing may not be able to identify a true trend in strength, the higher strength for the more polished samples could be due to such effects as stronger bonds due to the smoother finish and more dense coating or due to the more polished SiC material having fewer surface flaws. Optical micrographs of the fracture surfaces are shown in Figure 12. For the less polished set of joined discs, failure was in the SiC substrate rather than the bond. The bond was pulled out intact from the failing SiC substrate. For the more polished set of joined discs, failure was primarily in the SiC as failure started in one substrate crossed through the bond region and continued in the other SiC substrate.

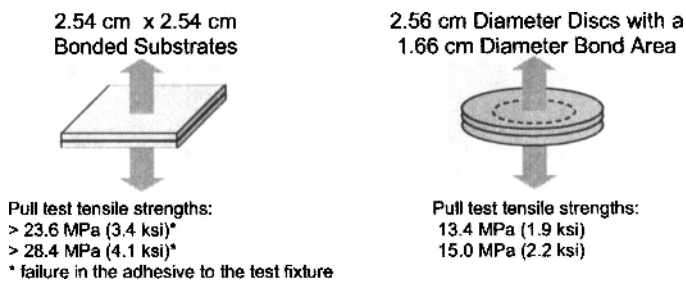


Figure 10. Illustration of the tensile tested samples and the resulting strengths.

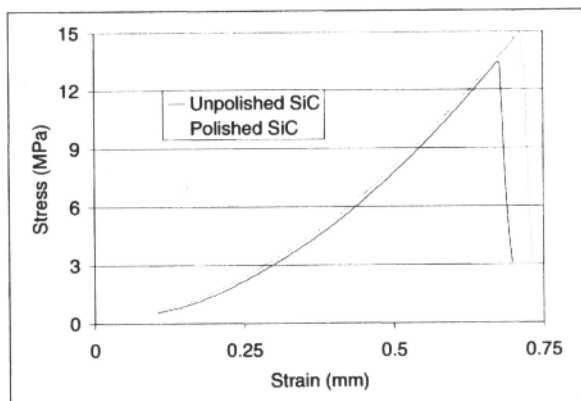


Figure 11. Stress versus strain curves for the two sets of joined discs.

The limitations of flaw identification with ultrasonic immersion were investigated through the analysis of joined Hexaloy SiC substrates that had simulated flaws and disbonds. The Ti foil interlayer had cut out shapes as shown in Figure 13a. The shapes were of circles, triangles, and squares. The widths/diameters of the shapes were 0.51 cm, 1.27 cm, 2.54 cm, and 3.81 cm. During processing of the bond, SiC bonding will only occur in regions where there is Ti. The general pattern of the flaws was distinguishable in the ultrasonic immersion results as seen in figure 13b. The simulated flaw areas appear as nonbonded regions. However, the resolution was much lower than for the bonded CVD discs that had a reduced bond area. The lower resolution is believed to be primarily due to the use of Hexaloy SiC which had three factors that could hinder good results in ultrasonic immersion. These factors are: thicker SiC substrates of 0.25" compared to the 60 mill thick CVD SiC, a lower density of 3.1 g/cm³ vs. 3.21 g/cm³ for the CVD SiC, and higher porosity (2-3% closed porosity) vs. no porosity for the CVD SiC

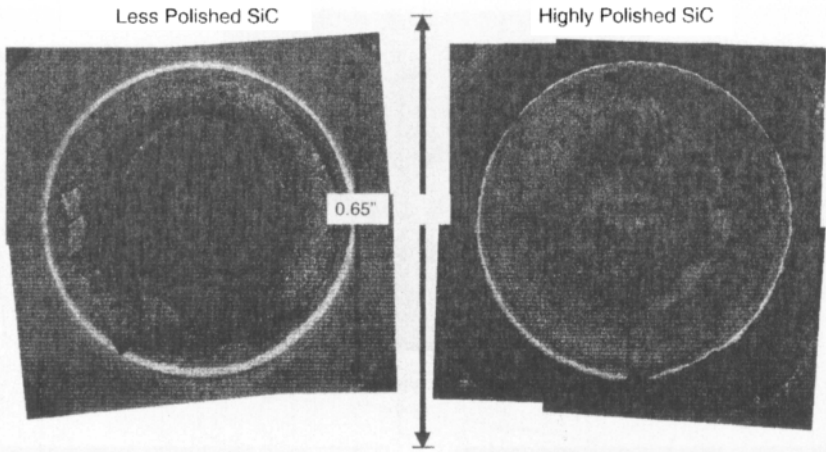


Figure 12. Optical micrographs of the failed surfaces in the tensile tested discs. Failure on the less polished set of discs is shown on the left and the failure for the more polished set of discs is on the right.

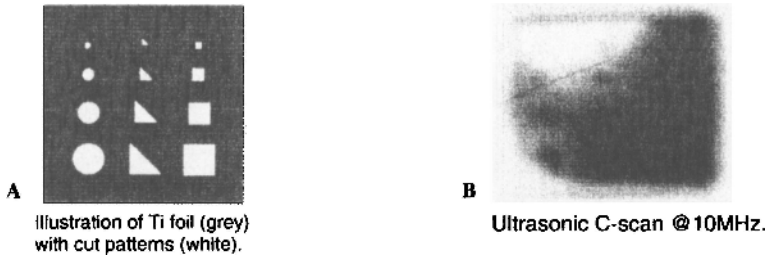


Figure 13a and 13b. Ultrasonic immersion of the bonded Hexaloy SiC with simulated flaws. An illustration of the Ti foil with cutout sections is shown in figure a. The resulting C-scan image from ultrasonic immersion is shown in figure b.

The diffusion bonds that were obtained from variations Ti interlayer thickness and diffusion bond processing times are shown in Figure 14 – 16. Figure 14 shows similar results for the diffusion bond formed from the 10 micron Ti foil at 2 hr as compared to one formed from the 10 micron PVD Ti coating at 2 hr (Figure 4). No microcracking was observed. For the 20 micron interlayer, an intermediate phase was observed in the core of the diffusion bond in the bond formed during the 2 hr hold. However the intermediate phase was not seen in the bond processed for 4 hr. For the bonds formed with the thick 50 micron Ti foil, microcracking, porosity, and the intermediate phase are observed as the processing time increased up to 16 hr. Future analysis with an SEM will further evaluate the diffusion bonds obtained in this study.

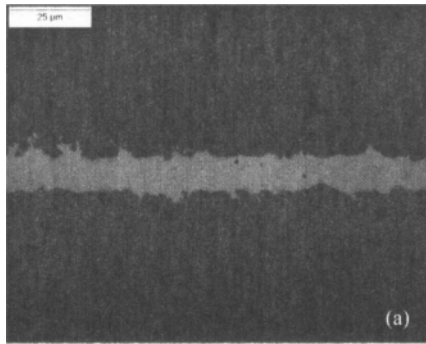


Figure 14. Optical micrograph of the SiC substrates joined with a 10 micron interlayer for 2 hr.

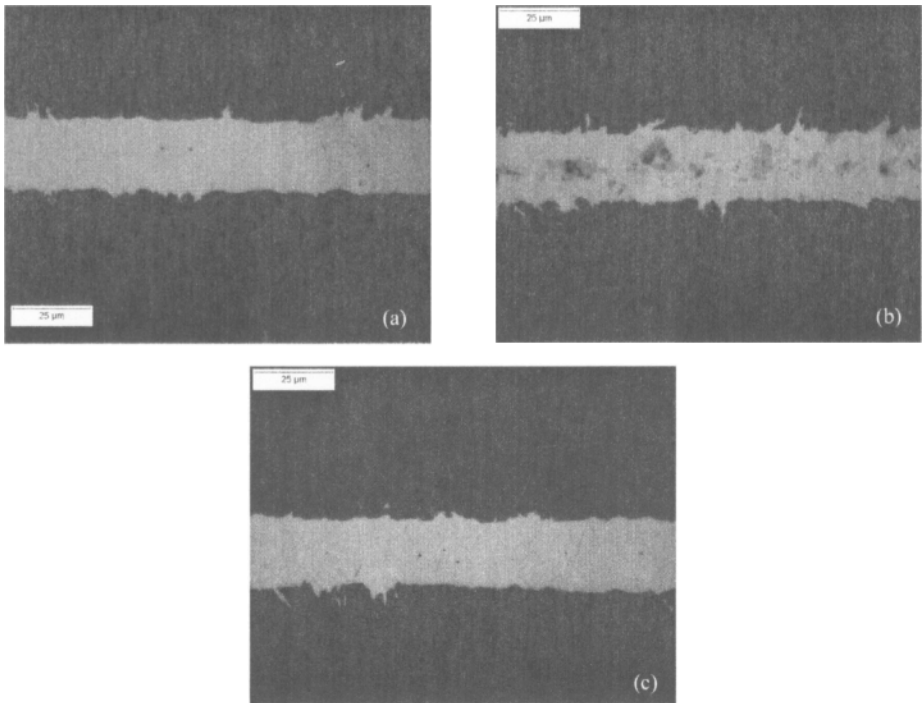


Figure 15. Optical micrographs of the SiC substrates joined with a 20 micron interlayer for 1 hr (a), a 20 micron interlayer for 2 hr (b), and a 20 micron interlayer for 4 hr (c).

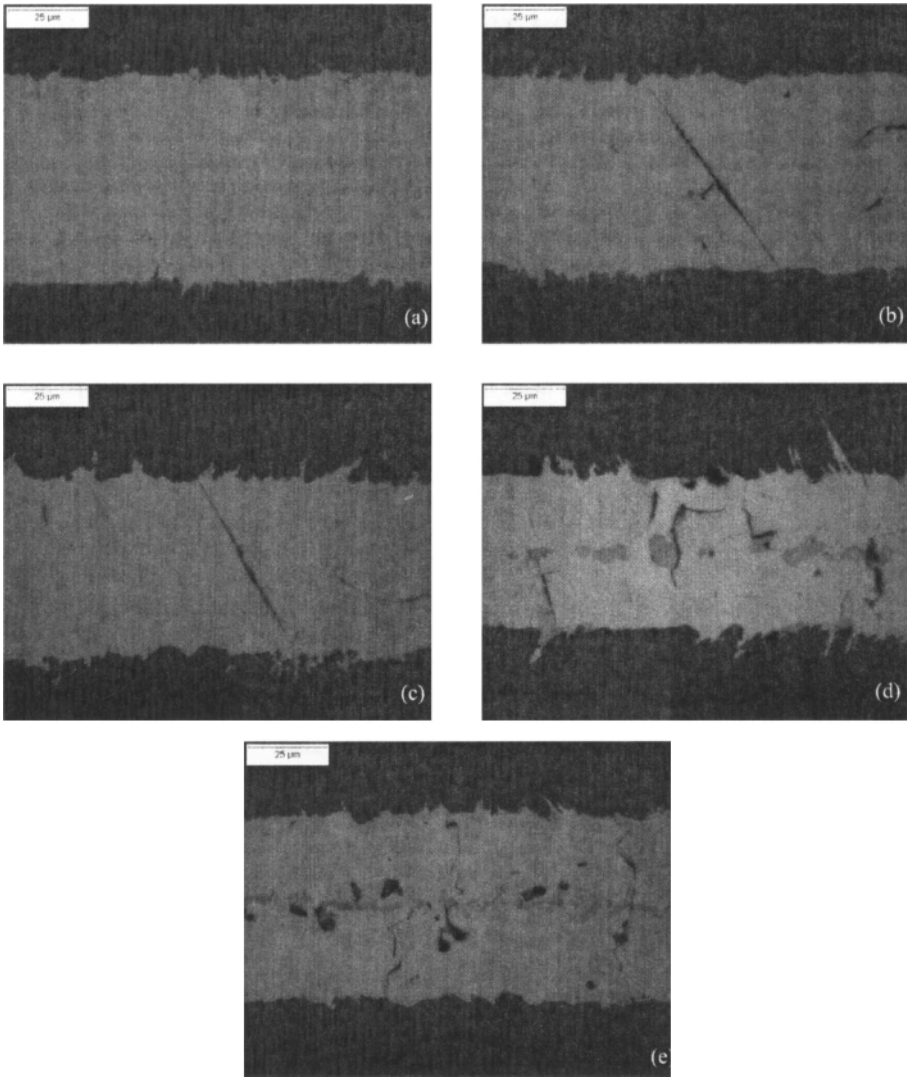


Figure 16. Optical micrographs of the SiC substrates joined with a 50 micron interlayer for 1 hr (a), a 50 micron interlayer for 2 hr (b), a 50 micron interlayer for 4 hr (c), a 50 micron interlayer for 8 hr (d), and a 50 micron interlayer for 16 hr (e).

CONCLUSIONS

A diffusion bonding approach that is well suited for fabricating a low emission ceramic injector was developed and characterized. Pure Ti interlayers were used to join SiC substrates. The resulting diffusion bonds were well adhered to the SiC substrates, with no delaminations. Microcracking was observed in some diffusion bonds due to the formation of $Ti_3Si_3C_4$ which is highly anisotropic in its thermal expansion. It was shown that microcracking could be avoided by preventing the formation of the intermediate phase of $Ti_3Si_3C_4$. The use of thin interlayers and longer processing times resulted in uniform, crack free bonds. The NDE method of ultrasonic immersion proved to be a very good method for analyzing the bond quality and for detecting small flaws and debonded areas. A polished surface finish was shown to have a positive effect on bond quality and strength compared to a more dull finish. The optimization of the processing of the diffusion bond and the resulting properties suggest that diffusion bonding is a good processing approach for fabricating complex shaped components.

ACKNOWLEDGEMENTS

This effort was supported by the NASA Glenn Research Center under the Subsonics Fixed Wing Project. The authors would like to thank James Smith for conducting microprobe analysis and Dr. Robert Okojie of NASA GRC for applying PVD Ti coatings. The authors would also like to thank Richard E. Martin and Laura M. Cosgriff of Cleveland State University for conducting NDE.

REFERENCES

1. R. Tacina, C. Wey, P. Laing, and A. Mansour, "A Low Lean Direct Injection, Multipoint Integrated Module Combustor Concept for Advanced Aircraft Gas Turbines," NASA/TM-2002-211347, April 2002.
2. M. C. Halbig, M. Singh, T. P. Shpargel, J. D. Kiser, "Diffusion Bonding of Silicon Carbide Ceramics Using Titanium Interlayers," Proceedings of the 30th International Conference & Exposition on Advanced Ceramics & Composites, Cocoa Beach, FL, Jan. 22-27, 2006.
3. M. C. Halbig, M. Singh, T. P. Shpargel, J. D. Kiser, "Diffusion Bonding of Silicon Carbide for MEMS- LDI Applications," Proceedings of the 31st International Conference & Exposition on Advanced Ceramics & Composites, Daytona Beach, FL, Jan. 21-26, 2007.
4. J. H. Schneibel, C. J. Rawn, E. A. Payzant, and C. L. Fu, "Controlling the Thermal Expansion Anisotropy of Mo_5Si_3 and Ti_5Si_3 Silicides," *Intermetallics*, **12**, 845-850 (2004).
5. J. H. Schneibel and C. J. Rawn, "Thermal Expansion Anisotropy of Ternary Silicides Based on Ti_5Si_3 ," *Acta Materialia*, **52**, 3843-3848 (2004).
6. L. Zhang and J. Wu, "Thermal Expansion and Elastic Moduli of the Silicide Based Intermetallic Alloys $Ti_5Si_3(X)$ and Nb_5Si_3 ," *Scripta Materialia*, **38**, 2, 307-313 (1998).
7. R. Boyer, G. Welsch, E.W. Colling, *Material Properties Handbook: Titanium Alloys*, ASM International, Materials Park, OH, 1994, p.p. 516.
8. J. W. Elmer, T. A. Palmer, S. S. Babu, E. D. Specht, "In Situ Observations of Lattice Expansion and Transformation Rates of α and β Phases in Ti-6Al-4V," *Materials Science and Engineering A*, **391**, 2005, pp. 104-113.
9. M. Naka, J. C. Feng, and J. C. Schuster, "Phase Reaction and Diffusion Path of the SiC/Ti System," *Metallurgical and Materials Transactions A*, **24A**, 1385-1390, (1997).